ANL-6281

Argonne National Laboratory

SHIELD DESIGN METHODS FOR ARGONAUT-TYPE REACTORS

by

John Fagan

DISCLAIMER

Price $1.00 . *Available from the Office of Technical Services, Department of Commerce, Washington 25, D.C.*

ANL-6281
Reactor Technology
(TID-4500, 16th Ed.)
AEC Research and
Development Report

ARGONNE NATIONAL LABORATORY
9700 South Cass Avenue
Argonne, Illinois

SHIELD DESIGN METHODS FOR ARGONAUT-TYPE REACTORS

by

John Fagan

March 1960

Operated by The University of Chicago
under
Contract W-31-109-eng-38

TABLE OF CONTENTS

LIST OF FIGURES

LIST OF TABLES

SHIELD DESIGN METHODS FOR ARGONAUT-TYPE REACTORS

by

John Fagan

ABSTRACT

The methods used in calculating the shielding for Argonaut-type reactors are described. The shield designs for the Argonaut-I Reactor, now operated by the International School of Nuclear Science and Engineering at Argonne National Laboratory, and the Argonaut Reactor, which was displayed at the Second United Nations International Conference on the Peaceful Uses of Atomic Energy, Geneva, 1958, were investigated. The methods used appeared to be satisfactory within the anticipated limits of accuracy.

INTRODUCTION

There are almost as many approaches to the shielding of stationary nuclear reactors as there are people in the business. This situation is a result of several things. One is surely the newness of this field, but probably more important is the fact that the requirements of accuracy are not very stringent in many cases. If one notes that three inches of iron, nine inches of high-density concrete, or 1 foot of ordinary concrete change the dose rate at the outside of a shield by a factor of approximately 10, then it is easy to see why many people advocate simply adding this amount to the outside of a shield structure which may already be 6, 10, or even 15 feet thick. Upon accepting such a philosophy with regard to the engineering design of a nuclear reactor shield, the objective then becomes to produce a method which will predict simply and rapidly the radiation dose rates to within, let us say, a factor of two.

This report presents a method which shows possibilities of doing just that sort of job. The approach is one in which shielding design data may be obtained within a reasonable length of time by means of hand calculations (and obviously much more rapidly if a digital computer is used). An attempt has been made to present as completely as possible the computational schemes and the necessary assumptions as they apply to the Argonaut system. Limited experimental data have been obtained, and a comparison of the experimental and measured values of the dose rates is given in the final section of this report.

Two similar shield designs were investigated: that for the Argonaut I[1,2] and that for the Argonaut-G,[3] built for the United States display in the 1958 Geneva Conference.

The Argonaut-type reactors are heterogeneous thermal reactors designed to operate at a maximum intermittent power of 10 kw. The Argonaut was designed as an inexpensive, but highly flexible, low-power reactor for university research and instruction. In order that these low-power reactors might be shielded inexpensively, ordinary concrete blocks, both with and without iron slugs in the mixture, were selected. In addition, boral sheets and laminated Masonite and iron were used to obtain the maximum shielding where space was limited.

In all cases the calculations were made for the most pessimistic case of a one-slab loading on the side of the core nearest the direction of the shielding being calculated. The calculations were normalized to a 10-kw thermal power level for both reactors, which gave an average thermal neutron flux in the core of 10^{11} n/(cm^2)(sec).

A schematic description of the shields is given in Figures 1 and 2 to show a cross section of the materials and distances used in shielding the reactors in the direction of the four centerline calculations. A view of the Argonaut I is given in Figure 3.

SHIELD DESCRIPTION FOR THE GENEVA ARGONAUT

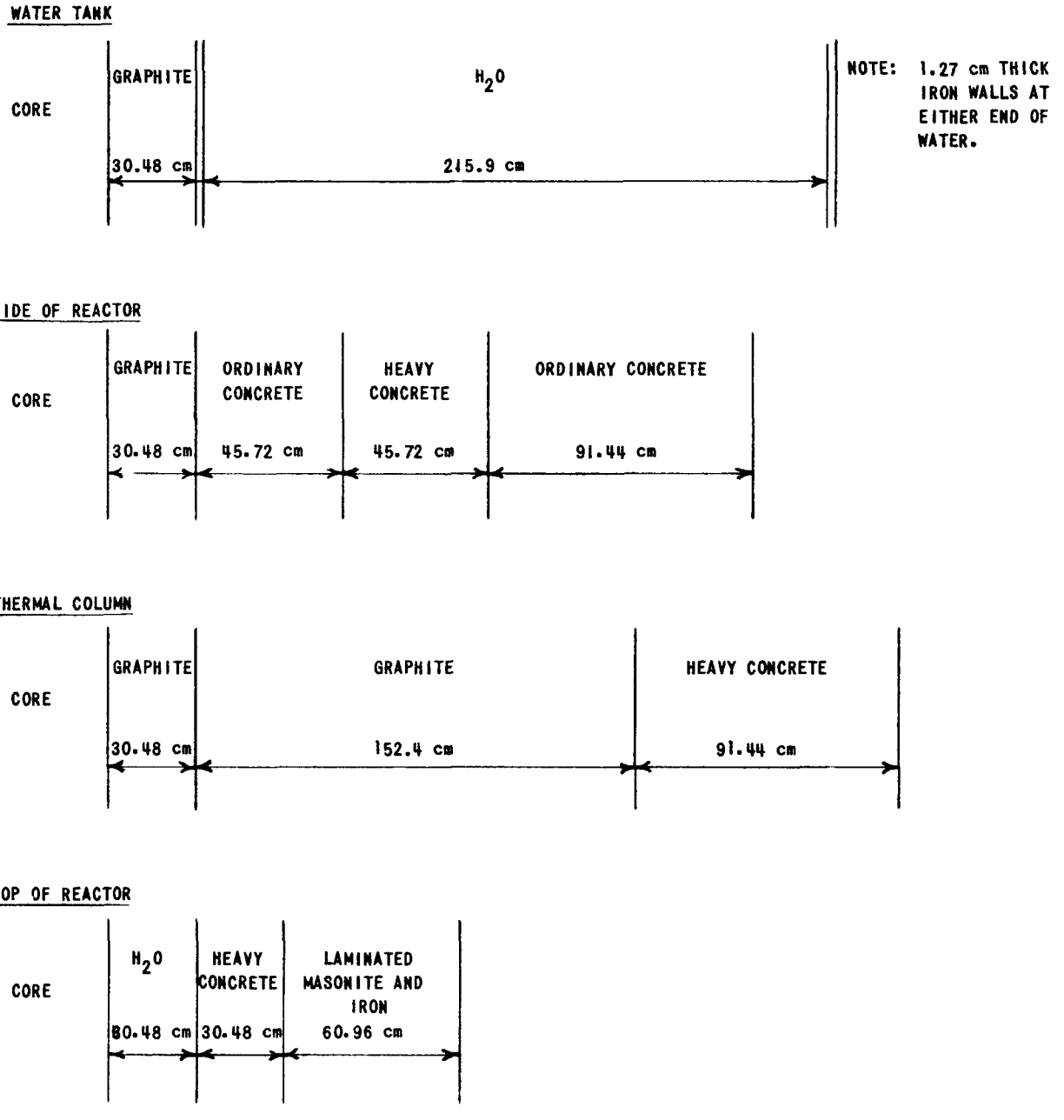

FIGURE 1

SHIELD DESCRIPTION FOR ARGONAUT-I

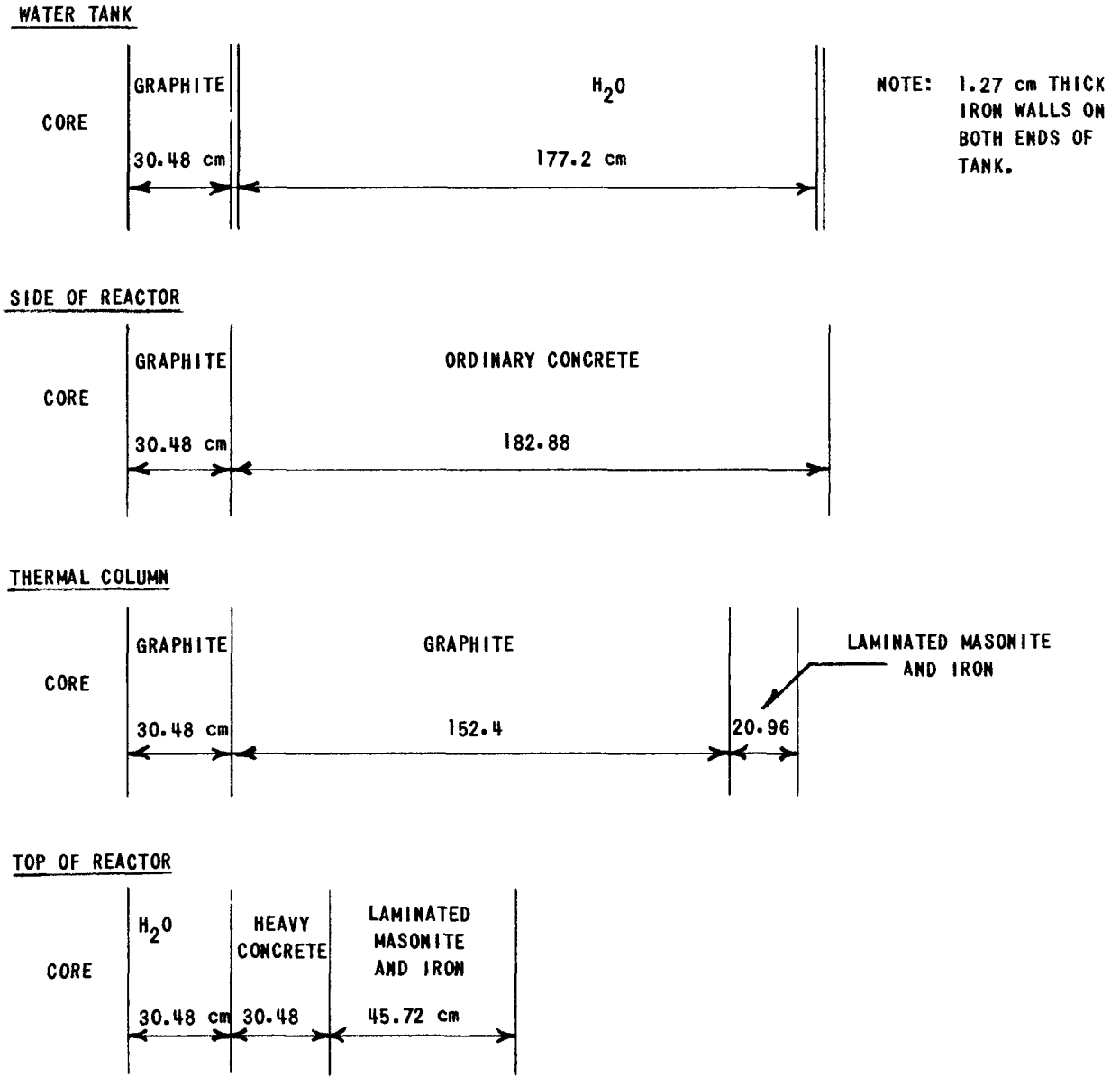

FIGURE 2

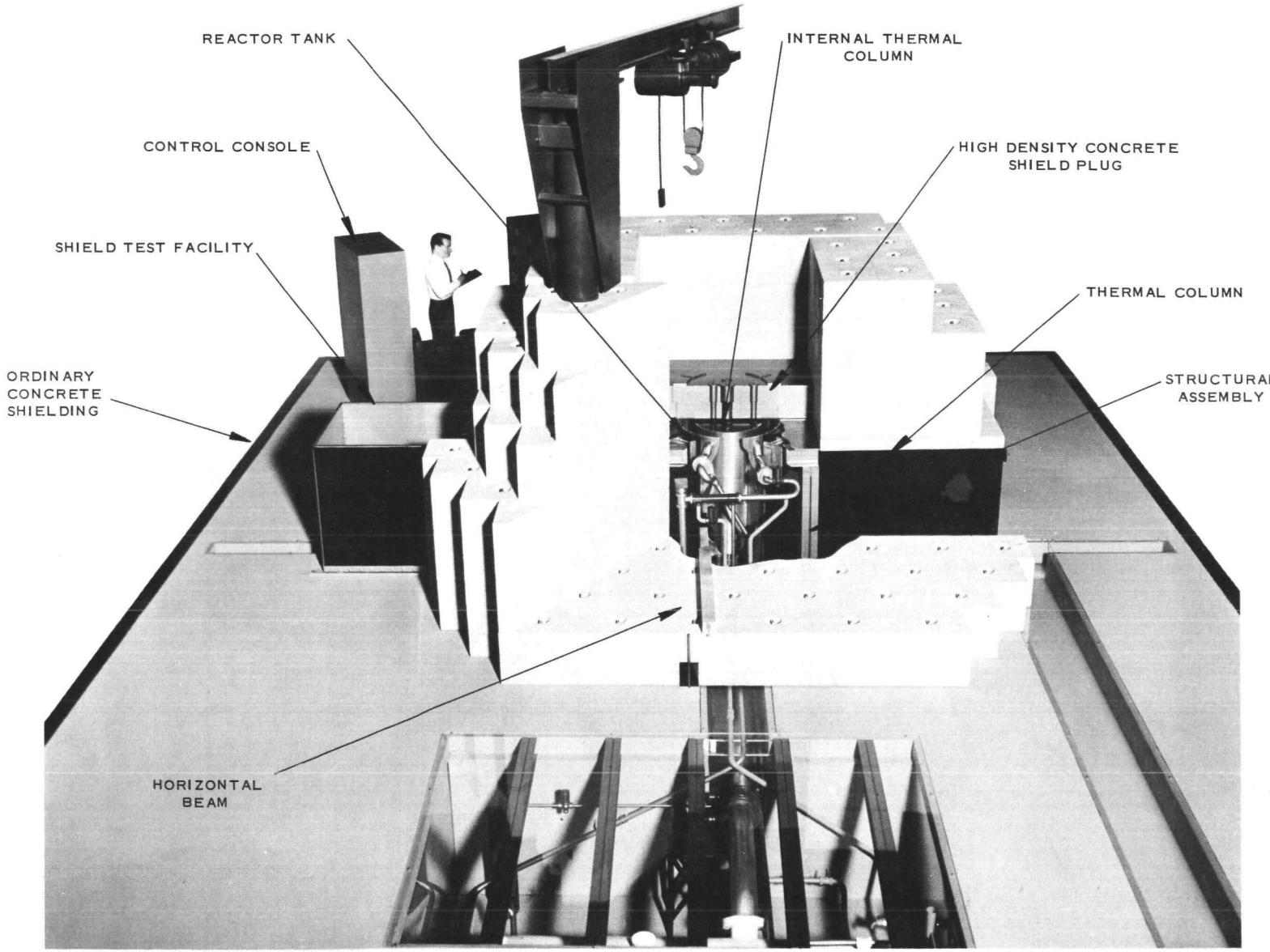

FIG. 3

CUTAWAY MODEL OF ARGONAUT REACTOR

NOMENCLATURE

$\overline{A}$ - Average atomic weight

a - Distance from outside of core to point of evaluation

α, β, γ - Buckling constants

B - Buildup factor

b - Number of mean free paths

β - Buckling in the horizontal direction

C - Correction factor

D - Diffusion coefficient

D_s - Thermal diffusion coefficient

h - Height

K, κ - Constant in diffusion equation

L - Diffusion length

λ_{tr} - $1/\Sigma_{tr}$, mean free path (transport)

M - A parameter

μ - Gamma-ray attenuation coefficient

ν - κ/μ

ϕ - Flux

Q_2 - Neutron or gamma-ray source per unit area and time, n or $\gamma/(cm^2)(sec)$

Q_3 - Neutron or gamma-ray source per unit volume and time, n or $\gamma/(cm^3)(sec)$

R - Radius

ρ - Density, gm/cm^3

Σ_a - Macroscopic cross section for absorption

Σ_i - Slope of fast neutron flux in region i

Σ_r - Macroscopic fast removal cross section

Σ_s - Macroscopic cross section for scattering

Σ_{tr} - Macroscopic transport cross section

V_i - Volume fraction of component i

x - Distance

Z - Self-absorption distance

$\overline{Z}$ - Average atomic number

METHODS OF CALCULATION

An investigation of the fission process shows that there are many particles given off when a nucleus is cracked. Among these are the fission fragments, alpha particles, electrons, positrons, deuterons, tritons, neutrons, neutrinos and gamma rays. All of the charged particles and fission fragments can be neglected immediately because of their very short ranges compared to those of the neutron, neutrino, and gamma ray. Of these three neutral particles, the effect of the neutrino is negligible because of its extremely long range. The average neutrino passes through a distance equal to the diameters of 10^8 stars the size of our sun before interacting with matter. Therefore, the particles of concern in shielding are the neutron and the gamma ray.

All the neutrons are a direct result of fission and consequently are born in the core of the reactor. The gamma rays are produced in several ways. Prompt fission gamma rays are emitted at the instant of fission and thus also are all born in the core. Equilibrium fission product gamma rays are also born in the core of the reactor. However, they are not given off at the instant that fission occurs, since they result from the decay of fission products. The equilibrium fission product gamma rays can be treated in exactly the same manner as are the prompt fission gamma rays since they reach an equilibrium value after the reactor has been in operation for a short time. A third source of gamma rays, capture gamma rays, carry off a portion of the kinetic energy of the neutron when it is captured or absorbed in a material and thus are born throughout the shield.

The first consideration in the model proposed herein[11] is to determine the neutron distributions throughout the shield. At this point several assumptions are made. First, a modified one-group approach is used to obtain the distribution of thermal neutrons in the shield. In this model the diffusion equation is solved with a source term which represents the slowing down of fast neutrons into the thermal group. The thermal source term is the loss of neutrons from the fast or uncollided neutron flux. The uncollided flux is found in general by integrating a point kernel over the source volume, making use of the removal cross section to attenuate the flux through the intervening material.[10,11] The actual integrations have been shown frequently in the literature and the resulting equations for the appropriate geometries were obtained from Rockwell.[12]

The calculation of the prompt fission product and the equilibrium fission product gamma-ray fluxes at the outside of the shield is accomplished in much the same manner as that of the uncollided neutron flux except that the total attenuation coefficient for gamma rays replaces the removal cross section and an appropriate buildup factor is used.

After having treated all of the sources of radiation from the core in the manner described above, the problem of determining the gamma-ray flux due to capture gamma rays must be handled. The shield is effectively broken into regions which contain only one material and in which the thermal neutron flux can be approximated by a single exponential attenuation. The kernel approach is again used with the appropriate attenuation coefficients and buildup factors to obtain the gamma-ray flux at the outside of each region. The flux at the outside of each of these regions is then treated as a plane source and attenuated through the remainder of the shield to get the flux at the outside of the shield. The distribution in energy of the gamma rays is taken into account by approximating the true energy spectrum by a line spectrum which groups the gamma rays into discrete segments with average energies.

The details of the calculations as they apply to the Argonauts are presented below, beginning with the uncollided neutron flux calculations, continuing through the capture gamma-ray calculations, and including the conversion of fluxes to dose rates and the summing of the dose rates at various energies to get the total predicted dose rate at the outside of the shield. Samples of each type of calculation are shown, including the sources of the constants used.

Constants

Obtaining the constants to use in a shielding problem such as is being treated here presents many difficulties. The simplest approach possible was used to obtain unknown material constants. A similar material with known constants was found and these constants were attributed to the material in question. The thermal neutron constants for the elements and for water were taken from Nucleonics Data Sheet No. 8.[4] The removal cross sections for fast neutrons were obtained from Chapman and Storrs.[5] The constants for the core, heavy concrete, and the laminated Masonite and iron region were calculated by weighting the component material constants by their respective fractions and summing to get the regional constant (see Table I). The ordinary concrete was found to be similar to type 03 concrete[6] and the constants for the latter were used. The gamma-ray attenuation coefficients were those of Grodstein.[7] The buildup factors for all materials, except Masonite, were taken from ANL-5800[8] and NYO-3075,[9] the assumption being made that the buildup for graphite could be approximated by the buildup for aluminum. The average atomic number, $\overline{Z}$, for the Masonite and iron mixture was found to be similar to that of aluminum; therefore, the values of buildup for aluminum were used for that material also.

Table I

NUCLEAR CONSTANTS FOR MATERIALS USED

Material	$\Sigma_r(cm^{-1})$	$D_s(cm)$	L(cm)	$\kappa(cm^{-1})$	$\Sigma_a(cm^{-1})$
Water	0.0977	0.164	2.73	0.366	0.022
Aluminum	0.0790	5.52	20.0	0.050	0.014
Graphite	0.0602	0.778	54.4	0.0184	2.6×10^{-4}
Ordinary Concrete	0.0860	0.558	7.87	0.127	8.95×10^{-3}
Heavy Concrete	0.102	0.698	3.94	0.254	0.0600
Core	0.0792	-	-	-	0.0752
Uranium	0.168	-	-	-	-
Iron	0.150	1.27	-	-	0.192
Masonite	0.130	0.617	-	-	0.0154
Homogenized Masonite and Iron	0.140	0.943	-	-	0.104

Sample Calculation of Constants for Mixtures

The Masonite was assumed to have a density of 1.3 gm/cm^3. Its composition was taken as 0.078 gm/cm^3 of hydrogen, it being assumed that the remainder was approximately one-half carbon and one-half oxygen, that is, there are 0.611 gm/cm^3 of carbon and 0.611 gm/cm^3 of oxygen. Accordingly, the atomic composition was calculated to be

$0.078/1.008 = 0.077$ gm-atom/$cm^3 = 4.64 \times 10^{22}$ atoms/cm^3 hydrogen;

$0.611/12 = 0.0509$ gm-atom/$cm^3 = 3.07 \times 10^{22}$ atoms/cm^3 carbon; and

$0.611/16 = 0.0382$ gm-atom/$cm^3 = 2.30 \times 10^{22}$ atoms/cm^3 oxygen.

The constants for Masonite were then calculated from the equation

$$\Sigma_s = V_H(\Sigma_s)_H + V_C(\Sigma_s)_C + V_O(\Sigma_s)_O$$

Thus

$$(\Sigma_s)_M = (0.0464)(7.0) + (0.0307)(4.8) + (0.023)(4.2)$$

$$= 0.325 + 0.147 + 0.0966 = 0.568 \text{ cm}^{-1} \quad .$$

Then

$$\lambda_{tr} = \frac{1}{(\Sigma_s)\left(1 - \frac{2\bar{A}}{3}\right)} = \frac{1}{(0.568)[1-(2/3)(13)]} = 1.85 \text{ cm} \quad ,$$

where $\bar{A}$ is the average atomic weight. Then

$$D_s = \lambda_{tr}/3 = 1.85/3 = 0.617 \text{ cm}$$

and

$$\Sigma_a = V_H(\Sigma_a)_H + V_C(\Sigma_a)_C + V_O(\Sigma_a)_O$$

$$= (0.0464 \times 10^{24})(0.33 \times 10^{-24}) + (0.0307)(0.0032) + (0.0230)(0)$$

$$= 0.0153 + 0.000098 = 0.0154 \text{ cm}^{-1} \quad .$$

Fast Neutron Flux.

The concept of the fast removal cross section[10,11] was used to calculate the attenuation of fast neutrons through the shield. The fast neutron fluxes through the three horizontal directions of the reactor (that is, the concrete side, the thermal column, and the water tank) were computed as the flux from a finite cylindrical source.[12] The size of the cylinder was determined by the diameter of the outside tank of the annular fuel region and the height of the fuel plates. The source strength of a one-slab fuel loading operating at 10 kw was attributed to the whole cylinder.

The use of the whole cylinder as a source to represent the true fuel region, which was only about one-quarter of a 6-in. thick annulus, seemed at first questionable. Therefore, additional calculations for the contribution to the flux in the shield of the central region and the part of the annulus where there is no fuel were made. The central region contributed only about 10 per cent of the flux at any point in the shield and thus could be neglected. The contribution of the remaining three-quarters of the annulus was also found to be negligible. When making calculations of the fast neutron flux in the direction of the water tank, the Bulk Shielding Facility Pure Water Data Work Sheet[13] was used. The first few

centimeters of the region outside the core were not handled as in the Bulk Shielding Facility, since this region in the water tank data represented the high thermalization of the fission neutrons, and in the Argonaut reactors the neutrons had already passed through one foot of graphite moderator.

For the calculation of the fast neutron flux through the top of the reactor, the fuel region was quite reasonably represented by three smaller cylinders placed side by side in the annular fuel region. The sizes of the cylinders were determined by the heights of the fuel elements and the total volume of the fuel region. For purposes of calculation, the cylinders were replaced by discs at the top of the cylinders.[14] The area source term for the discs was obtained by calculating the flux at the surface of an infinite half-space. This was a pessimistic representation of the flux at the top surface of the cylinders. The flux throughout the shield was then evaluated for the first five mean free paths by determining the contribution of the three discs on the centerline of the central disc. Beyond the five mean free paths, the contribution from each of the discs was essentially the same, and so the contribution from the central disc was evaluated and multiplied by three.

Sample Calculations of Fast Neutron Flux

The fast neutron flux distribution through the graphite in the direction of the water tank is given by

$$\phi(a) = \frac{Q_3 R_0^2}{2(a+Z)} F(\theta, b_2) \quad ,$$

where

Q_3 = average fast neutron source in the core, $n/(cm^3)(sec)$

R_0 = radius of assumed core cylinder

Z = self-absorption distance

m = parameter used in determining Z

$b_1 = a(\Sigma_r)_{graphite}$

a = distance from outside of core to point of evaluation

$b_2 = b_1 + (\Sigma_r)_{core}\ (Z)$

h = height of core = 60.96 cm

$F(\theta, b_2)$ is as given in TID-7004, p 348 (ref. 14).

The above equation was evaluated in the tabular form shown below to obtain the fast neutron flux distribution:

a, cm	a + R_0, cm	$(\Sigma_r)_{core}$ x (a + R_0)	a/R_0	m	b_1	$(1/m)(\Sigma_r)_{core}Z$	$(1/m)(\Sigma_r)_{core}$, cm^{-1}
0	45.7	3.62	0	0.80	0	2.32	0.0990
30.5	76.2	6.03	0.667	1.07	1.83	1.97	0.0743

Z, cm	a + Z, cm	$(\Sigma_r)_{core}Z$	b_2	$\frac{h/2}{a+Z}$	θ	$F(\theta,b_2)$	$\frac{F(\theta,b_2)}{a+Z}$, cm^{-1}	$\frac{Q_3R_0^2}{2}$, $n_f/(cm)(sec)$
23.4	23.4	1.59	1.86	1.18	49.7	0.100	4.27×10^{-3}	1.36×10^{13}
26.5	57	2.10	3.93	0.511	27.1	7.6×10^{-3}	1.33×10^{-4}	1.36×10^{13}

ϕ, $n_f/(cm^2)(sec)$	a, cm
5.81×10^{10}	0
1.81×10^{9}	30.5

The Bulk Shielding Facility Data were used to determine the fast neutron distribution in the water tank:

$$\phi(a) = 1.18 \times 10^9 \, (\phi_2/\phi_1)$$

from values of

x = distance from inner interface of region to point of evaluation

$\phi(a)$ = fast neutron flux in water tank evaluated at a cm from reactor core

ϕ_1 = fast neutron flux per unit power on data sheet at 30 cm from beginning of water = 9.0×10^3 $n/(cm^2)(sec)(watt)$

ϕ_2 = fast neutron flux per unit power on data sheet at x + 30 cm from beginning of water.

This calculation was carried out again in a tabular form as shown below:

x, cm	a, cm	x + 30, cm	ϕ_2 at x + 30, $n/(cm^2)(sec)(watt)$	ϕ_2/ϕ_1 from Data Sheet	$\phi(a)$, $n_f/(cm^2)(sec)$
0	31.8	30	9.0×10^3	1	1.18×10^9
100	131	130	2.7×10^{-2}	3.0×10^{-6}	3.54×10^3

Fast neutron flux in direction of top of reactor.

The calculation of the source per unit area is as follows

$$Q_2[n/(cm^2)(sec)] = \frac{Q_3[n/(cm^3)(sec)]}{2\Sigma_r\ [cm^{-1}]} E_2(0) = \frac{Q_3}{2\Sigma_s}\ [n/(cm^2)(sec)]$$

$$= \frac{1.30 \times 10^{10}}{2\,(0.0792)} = 8.22 \times 10^{10}\ n/(cm^2)(sec)$$

where $E_2(0)$ is the exponential integral of the second order.

The equation expressing the fast neutron flux from single disc, A, on centerline of that disc is as follows:

$$\phi_A(a) = \frac{Q_2}{2}[E_1(b_1) - E_1(b_1 \sec\theta)] \quad .$$

This was evaluated in tabular form to obtain the flux through the top of the reactor, as shown below, where θ is the angle subtended by the source and E_1 is the exponential integral of the first order.

a	x_1	x_2	$\mu_1 x_1$	$\mu_2 x_2$	b_1	R_0/a	θ	$\sec\theta$	$b_1 \sec\theta$
5	5.0	0	0.489	0	0.489	1.97	63.1	2.21	1.08
40	30.5	9.52	2.98	0.971	3.95	0.246	13.8	1.03	4.07

$E_1(b_1)$	$E_1(b_1 \sec\theta)$	$E_1(b_1) - E_1(b_1 \sec\theta)$	$\phi_A(a)$, $n/(cm^2)(sec)$
0.57	0.200	0.37	1.52×10^{10}
4.0×10^{-3}	3.5×10^{-3}	5.0×10^{-4}	2.06×10^{7}

The equation expressing the fast neutron flux from two discs, B, on either side of the center disc is as follows:

$$\phi_B(a) = \frac{2Q_2}{2}[E_1(b_1) - E_1(b_1 \sec\theta)]\,[C(d/R_0,\ a/R_0,\ \bar{\mu}R_0)]$$

where

C = correction factor for evaluation off centerline of disc

$\bar{\mu}$ = average attenuation coefficient in shield

d = radius of disc.

Evaluation was done in tabular form as shown below:

a/R_0	a_1, cm	d/R_0	$\bar{\mu}$, cm^{-1}	$\bar{\mu}R_0$	C	x_1	x_2	M_1x_1	M_2x_2	b_1
0.25	2.46	2.0	0.0977	0.961	0.050	2.46	0	0.240	0	0.240

$R_0/a = \arctan\theta$	$\sec\theta$	$b_1 \sec\theta$	$E_1(b_1)$	$E_1(b_1 \sec\theta)$
4.0	4.12	0.990	1.0	0.23

$E_1(b_1)-E_1(b_1 \sec\theta)$	$\phi_B(a)$, $n/(cm^2)(sec)$
0.77	3.17×10^9

Therefore, the flux as a function of a is

$$\phi_F(a) = \phi_A(a) + 2\,\phi_B(a) \quad .$$

Evaluating at a = 20 cm,

$$\phi_F(20) = \phi_A(20) + 2\,\phi_B(20) = 6.16 \times 10^8 + 3.2 \times 10^8 = 9.36 \times 10^8\ n/(cm^2)(sec) \quad .$$

Thermal Neutron Flux

A one-group diffusion equation with the source term defined to be the loss from the fast group was used to evaluate the thermal neutron distribution. The fast neutron flux was described in the previous section and the loss from that group, which would be the negative divergence of the fast neutron current, can be approximated by the product of the removal cross section and the fast neutron flux at any point. Thus, the equation to be solved is

$$D_s \nabla^2 \phi_s(x) - \Sigma_a\, \phi_s(x) + \Sigma_r\, \phi_f(x) = 0 \quad .$$

Assuming a single exponential form of the fast flux $\phi_f(x)$ in each region and solving in infinite slab geometry yields

$$\phi_s(x) = A\,e^{Kx} + Be^{-Kx} + Ce^{-\Sigma_r x} \quad ,$$

where

$$K^2 = \Sigma_a / D_s$$

$$C = \Sigma_r \, \phi_f(0) / D_s (K^2 - \Sigma_r^2)$$

Σ_r = slope of ϕ_f on a semilog plot

and A and B are arbitrary constants to be determined by the boundary conditions. The boundary conditions used in evaluating A and B for each region in the thermal neutron equations were: first, the value of the flux at the inside of the innermost region; second, matching the flux, ϕ, at the interface between regions; third, matching the current, J, at the interface between regions; and fourth, specifying the flux to be zero either at infinity or at the extrapolated distance in the outermost region. The thermal neutron fluxes in the water tank for each reactor and the side of the Argonaut I reactor were calculated in the manner described above.

In the case of the thermal columns for both reactors, it was felt that the approximation given by infinite slab geometry could be improved by a buckling correction which was used to account for the loss of neutrons due to leakage through the sides.[16] The correction which was applied can be derived from the diffusion equation in a nonmultiplying medium. The solution of the diffusion equation

$$\nabla^2 \phi_{th} + K^2 \phi_{th} = 0$$

in Cartesian coordinates yielded

$$\phi_{th}(x,y,z) = EFG \cos(\alpha x)\cos(\beta y) \, e^{-\gamma z}$$

(having already applied the boundary condition of the flux going to zero at infinity).

Considering the centerline flux,

$$\phi(z) = EFG \, e^{-\gamma z}$$

where $\gamma^2 = K^2 + \alpha^2 + \beta^2$, which can be seen from the equation obtained by separating the variables;

$$\frac{x''}{x} + \frac{y''}{y} + \frac{z''}{z} + K^2 = \alpha^2 + \beta^2 - \gamma^2 + K^2 = 0 \quad .$$

Therefore,

$$\phi(z) = EFG\, e^{-(K^2 + \alpha^2 + \beta^2)^{1/2} z} \quad .$$

Now, examine the infinite slab solution for one region with flux going to zero at infinity:

$$\phi(x) = Ae^{-\kappa x} + Ce^{-\Sigma_r x} \quad .$$

In a region with no source from the fast group, the constant C equals zero and the second term is eliminated. Therefore, the flux equation is

$$\phi = Ae^{-\kappa x}$$

and, by comparison with the attenuation in finite geometry when there is no source term,

$$\kappa = (K^2 + \alpha^2 + \beta^2)^{1/2} \quad .$$

Since K^2 equals Σ_a/D_{th}, it can be seen that the increase in the attenuation coefficient can be calculated from the buckling constants. This result is extrapolated to replace κ by $(K^2 + \alpha^2 + \beta^2)^{1/2}$ in the sum $Ae^{\kappa x} + Be^{-\kappa x} + Ce^{-\Sigma_r x}$, since the modification applies only to the leakage and the leakage loss should be independent of whether a source or nonsource region is considered.

The same sort of analysis can be made for cylindrical geometry, and it can be shown that κ^2 should be increased by α^2, the buckling in the radial direction. This correction was made in one of the trial methods used for the top of the reactor and is described below.

In the case of several regions, the calculation of the thermal neutron flux becomes quite cumbersome due to the large numbers of unknowns which must be determined. Therefore, machine calculations were used in several of the computations. The IBM-704 program RE-34[17] which was used solves the diffusion equation with a source term defined to be the product of the fast neutron flux and the removal cross section. In the machine calculations, a point-by-point source term was used; therefore, an analytical description of the fast flux was not necessary as it was for the hand computation. Also, the machine calculation could be done in slab, cylindrical, or spherical geometry, whereas the hand computation was limited to slab geometry. (Note: A comparison was made and it was found that the difference between the slab and cylindrical calculations was negligible for the configuration used in these problems.)

Again, as for the fast flux, the top of the reactor presented a very different picture than the horizontal directions for calculating the thermal neutron fluxes. Three trial methods were evaluated to determine the best approach. First, a spherical problem was solved for a source region of the same volume as the one-slab fuel region. Second, an infinite slab calculation with the proper power density was made. It was hoped that these two problems would define the limits and would straddle the third approach, which made use of the buckling correction for cylindrical geometry, as described in the thermal column calculations. The determination of the buckling for the top of the reactor was much more difficult than for the thermal column, since it was not clear over what region to determine the buckling constants. It was assumed that the flux went to zero at the outside of a cylinder whose size was that of the core section of the reactor. When the results from the three methods were compared, it was found that the fluxes from the spherical and the cylindrical methods were almost identical, while the evaluation using the buckling correction gave a noticeably smaller thermal neutron flux. Therefore, it was decided that the method of calculating the buckling was too arbitrary. The spherical results were selected, since they were only slightly less than the infinite slab solution, which was known to be too large.

Sample Calculation of Thermal Neutron Flux

The thermal neutron flux calculations in the direction of the side of the reactor for Argonaut-I are shown below.

The fast neutron flux in the reflector and shield regions can be represented by single exponentials with respective slopes of $\Sigma_{graphite}$ and $\Sigma_{concrete}$.

$$\Sigma_{graphite} = \frac{2.303 \log \frac{2.54 \times 10^{9}}{2.07 \times 10^{10}}}{(5 - 25)} = (-0.115)\log(0.123) = +0.105 \text{ cm}^{-1}$$

$$\Sigma_{concrete} = \frac{(2.303) \log \frac{1.79 \times 10^{9}}{1.39 \times 10^{1}}}{(183)} = (0.0126)\log(1.29 \times 10^{8})$$

$$= + 0.102 \text{ cm}^{-1} \quad .$$

The thermal flux in the graphite region is

$$\phi_1(x) = A_1 e^{\kappa_1 x} + B_1 e^{-\kappa_1 x} + C_1 e^{-\Sigma_1 x} \quad ,$$

where subscript 1 refers to that region and

$$C_1 = \frac{\Sigma_1 \phi_{f1}(0)}{D_1 s (\kappa_1^2 - \Sigma_1^2)} = \frac{(0.105)(3.51 \times 10^{10})}{(0.778)(-1.07 \times 10^{-2})} = -4.44 \times 10^{11} \text{ n/(cm}^2\text{)(sec)} \quad .$$

Therefore,

$$\phi_1(x) = A_1 e^{(0.0184)x} + B_1 e^{-(0.0184)x} - (4.44 \times 10^{11}) e^{-(0.105)x} \quad .$$

The thermal flux in the concrete region is

$$\phi_2(x) = A_2 e^{\kappa_2 x} + B_2 e^{-\kappa_2 x} + C_2 e^{-\Sigma_2 x} \quad ,$$

where subscript 2 referes to that region and

$$C_2 = \frac{\Sigma_2 \phi_{f2}(0)}{D_{2s}(\kappa_2^2 - \Sigma_2^2)} = \frac{(0.102)(1.79 \times 10^9)}{(0.558)(0.00571)} = 5.74 \times 10^{11} \text{ n/(cm}^2\text{)(sec)} \quad .$$

Therefore,

$$\phi_2(x) = A_2 e^{(0.127)x} + B_2 e^{-(0.127)x} + (5.74 \times 10^{11}) e^{-(0.102)x} \quad .$$

The boundary conditions are

1. $\phi_1(x) \Big|_{x=0} = 1.014 \times 10^{11}$ n/cm^2)(sec)
2. $\phi_1(x) \Big|_{x=30.48} = \phi_2(x) \Big|_{x=0}$
3. $J_1(x) \Big|_{x=30\ 48} = J_2(x) \Big|_{x=0}$
4. $\phi_2(x) \Big|_{x=\infty} = 0$.

Applying boundary condition 4,

$$A_2 e^{+\infty} + B_2 e^{-\infty} + (5.74 \times 10^{11}) e^{-\infty} = 0.$$

Therefore $A_2 = 0$ and

$$\phi_2(x) = B_2 e^{-(0.127)x} + (5.74 \times 10^{11}) e^{-(0.102)x} \quad .$$

Applying boundary condition 1,

$$\phi_1(x)_{x=0} = A_1 e^0 + B_1 e^{-0} - (4.44 \times 10^{11}) e^{-0} = 1.014 \times 10^{11} \text{ n/cm}^2\text{)(sec)}.$$

Applying boundary condition 2,

$$A_1 e^{(0.0184)(30.5)} + B_1 e^{-(0.0184)(30.5)} - (4.44 \times 10^{11}) e^{-(0.105)(30.5)}$$

$$= B_2 e^0 + (5.74 \times 10^{11}) e^0$$

or

$$1.75\ A_1 + 0.571\ B_1 - B_2 = 5.92 \times 10^{11} \text{ n/(cm}^2\text{)(sec)} \quad .$$

Applying boundary condition 3,

$$+\frac{d\phi_1(x)}{dx}\bigg|_{x=30.48} = +\,(D_2/D_1)\,\frac{d\phi_2(x)}{dx}\bigg|_{x=0}$$

or

$$\frac{d\phi_1(x)}{dx} = (0.0184)\,A_1\,e^{(0.0184)x} - 0.0154\,B_1\,e^{-(0.0184)x}$$

$$+ (4.44 \times 10^{11})(0.105)\,e^{-(0.105)x}$$

$$= (0.127)\,B_2\,e^{-(0.127)x} - (0.120)(5.74 \times 10^{11})e^{-(0.120)x} \quad .$$

Evaluating and equating the currents,

$$(0.0322)\,A_1 - (0.0105)\,B_1 + (0.0911)\,B_2 = -4.39 \times 10^2\ n/(cm^2)(sec) \quad .$$

Solving the three simultaneous equations from boundary conditions 1, 2 and 3 by means of determinants yields

$$A_1 = -8.40 \times 10^{10}\ n/(cm^2)(sec)$$
$$B_1 = 6.29 \times 10^{11}\ n/(cm^2)(sec)$$
$$B_2 = -3.83 \times 10^{11}\ n/(cm^2)(sec)$$

Therefore, the thermal flux for Argonaut I in each region through the side of the reactor are

$$\phi_1(x) = (-8.40 \times 10^{10})\,e^{(0.0184)x} + (6.29 \times 10^{11})\,e^{-(0.0184)x}$$

$$-(4.44 \times 10^{11})\,e^{-(0.105)x}$$

$$\phi_2(x) = -(3.83 \times 10^{11})\,e^{-(0.127)x} + (5.74 \times 10^{11})\,e^{-(0.102)x} \quad .$$

The evaluation of the thermal flux in the Graphite Region is shown in tabular form below:

a, cm	κx	Σx	$e^{+\kappa x}$	$e^{-\kappa x}$	$e^{-\Sigma x}$
0	0	0	1	1	1
30.5	0.561	3.20	1.75	0.571	0.0408

$Ae^{\kappa x}$, $n/(cm^2)(sec)$	$Be^{-\kappa x}$, $n/(cm^2)(sec)$	$Ce^{-\Sigma x}$, $n/(cm^2)(sec)$	$\phi(x)$, $n/(cm^2)(sec)$
8.40×10^{10}	6.29×10^{11}	4.44×10^{11}	1.01×10^{11}
1.47×10^{11}	3.59×10^{11}	1.81×10^{10}	1.94×10^{11}

The thermal neutron flux calculations for the thermal column and the third method of calculating the thermal neutron flux for the top of the reactor differ from the previous calculation only in that each κ is corrected appropriately for the buckling.

The calculation of the buckling correction for the thermal column is shown below:

$$0.71\ \lambda_{tr} = (0.71)\ 3\ D_{th} = (0.71)(3)(0.558) = 1.19\ \text{cm} \quad .$$

Horizontal buckling, β:

$$\beta = \pi/2b \qquad \text{where } b = (1.52/2) + 1.19 = 77.2\ \text{cm}$$

$$\beta = \pi/2(77.4) = 0.0203\ \text{cm}^{-1} \quad .$$

Vertical buckling, α:

$$\alpha = \pi/2a \qquad \text{where } a = 124/2 + 1.2 = 63.2\ \text{cm}$$

$$\alpha = \pi/2(63.2) = 0.0250\ \text{cm}^{-1} \quad .$$

Therefore

$$K^2 = \kappa^2 + \alpha^2 + \beta^2 = 0.000338 + 0.000625 + 0.000412 = 1.38 \times 10^{-3}\ \text{cm}^{-2} \ .$$

Prompt and Delayed Gamma Rays:

The prompt fission gamma rays were calculated using the same geometrical approximations as the fast neutrons with the addition of a buildup to account for the scattering of the gamma rays. The source for the gamma-ray calculations was determined by use of the equilibrium fission product and prompt fission line-spectrum distributions as found in ANL-5800.[18]

Sample Calculation of Prompt and Fission Product Gammas

The calculations of the prompt and fission product gamma-ray fluxes are identical to the methods used for fast neutrons with the exception of the addition of appropriate buildup factors. Therefore, they are not shown in detail here.

Capture Gamma Rays:

The dose rates at the outside of the shield due to the capture gamma rays were calculated using the line-spectrum approximation of the energy distribution of the gamma rays from capture as found in the

Reactor Shielding Design Manual.[12] The capture gamma-ray calculations were done for infinite slab geometry and for an exponential thermal flux in several regions throughout the shield. The contribution from each region was then attenuated through the remainder of the shield to predict the dose at the outside. Since in some cases a machine calculation for the thermal flux had been done, so that an analytical expression for the thermal flux was not available, the shield was therefore considered to be broken up into regions where the thermal flux could be approximated by a single exponential (i.e., a straight line on a semilog plot).

Sample Calculation of Capture Gamma Rays

The calculation of the dose at the outside of the reflector due to 2-Mev capture gamma rays from the graphite reflector is shown below. Since the equations available[11] for capture gamma-ray calculation are in terms of the distance increasing from the point of evaluation to the point of origin of the particle, the thermal flux equations must undergo a change in variables so that the distance variable, "t" increases from the outside to the inside of each region (whereas the distance x had increased in the opposite direction). Since each term of the thermal flux equation is a single exponential, the corresponding term of the new equation is modified by changing the sign of the exponential, and the constant is obtained by evaluating the term at the outer edge of the region.

$$\phi_s = -(1.37 \times 10^{11})\, e^{+(0.0184)x} + (6.824 \times 10^{11})\, e^{-(0.0184)x}$$

$$= (4.44 \times 10^{11})\, e^{-(0.105)x} \quad .$$

The first term, $-1.27 \times 10^{11}\, e^{0.0184x}$, when evaluated at x = 30.5 cm, gives $-(1.37 \times 10^{11})\, e^{+(0.561)} = -2.40 \times 10^{11}\ \gamma/(cm^2)(sec)$. The new first term is then $-(2.40 \times 10^{11})\, e^{-(0.0184)t}$. Treated in the same manner, the second term, $(6.82 \times 10^{11})\, e^{-(0.0184)x}$, becomes $(3.89 \times 10^{11})\, e^{+(0.0184)t}$, and the third term, $-(4.44 \times 10^{11})\, e^{-(0.105)x}$, becomes $-(2.09 \times 10^{10})\, e^{+(0.0105)t}$. Thus

$$\phi'_s(t) = -(2.40 \times 10^{11})\, e^{-(0.0184)t} + (3.894 \times 10^{11})\, e^{(0.0184)t}$$

$$- (2.09 \times 10^{10})\, e^{+(0.105)t} \quad .$$

First Exponential Term:

$$\nu_1 = -0.250 = \kappa_1/\mu$$

$$\phi_\gamma = \frac{Q_3}{-2\kappa_1} \left\{ e^{-\kappa_1 t'} E_1(\mu_s t') - n(1-\nu_1) + \frac{-\kappa_1}{-\kappa_1 - \mu_s} \left[e^{(-\kappa_1 - \mu_s)t'} - 1 \right] \right.$$

$$\left. -E_1 [(+\mu_s t')(1-\nu_1)] \right\} \quad , \qquad \text{for } \nu < 1$$

$$\phi_{\gamma_1} = \frac{-1.87 \times 10^7}{-2(0.0184)} \left\{(0.571)(0.040) - (+0.230) + (0.206)(-0.935) - (0.0187)\right\}$$

and

$$\phi_1 = 5.09 \times 10^8 \left\{0.0228 - 0.230 - 0.192 - 0.0187\right\} = -2.13 \times 10^8 \, \gamma/(cm^2)(sec).$$

Second Exponential Term:

$$\nu_2 = +0.259 = \kappa_2/\mu$$

$$\phi_{\gamma_2} = \frac{3.04 \times 10^7}{2(0.0184)} \left\{(1.75)(0.040) - (-0.300) + (-0.350)(-0.800) - (0.088)\right\}$$

$$= (8.25 \times 10^8) \left\{0.0701 + 0.300 + 0.279 - 0.088\right\} = +4.63 \times 10^8 \, \gamma/(cm^2)(sec).$$

Third Exponential Term:

$$\nu_3 = +1.48 = \kappa_3/\mu$$

$$\phi_{\gamma_3} = \frac{1.63 \times 10^6}{2(0.105)} \left\{24.5(0.040) - (0.738) + (3.09)(1.82) + 2.0\right\}$$

$$= (7.76 \times 10^6) \left\{0.981 + 0.738 + 5.61 + 2.0\right\} = -7.24 \times 10^7 \, \gamma/(cm^2)(sec).$$

Thus

$$\Phi_\gamma = \frac{Q_3}{2\kappa_2} \left\{ e^{+\kappa_2 t'} E_1 (\mu_s t') - \ell n (\nu_2 - 1) + \frac{\kappa_2}{\kappa_2 - \mu_s} \left[e^{(\kappa_2 - \mu_s)t} - 1 \right] \right.$$

$$\left. + E_i \left[\mu_s t' (\nu_2 - 1)\right] \right\} \quad , \quad \text{for } \nu > 1 \ .$$

Therefore the dose at the outside of the graphite from the capture in the graphite is $\phi_\gamma(\text{total}) = 1.79 \times 10^8 \, \gamma/(cm^2)(sec)$.

CALCULATED RESULTS

The results cited in Tables II and III include the calculated gamma-ray dose rates, the fast neutron fluxes, and the thermal neutron fluxes at the outside of the reactor shields on the core centerline, along with a breakdown of the major contribution to the gamma-ray dose rates. In addition, the centerline fast* and thermal neutron fluxes are shown in Figures 4, 5, 6 and 7 throughout the four shield directions of each reactor.

Table II

GAMMA-RAY DOSE RATES AND NEUTRON FLUXES AT THE OUTSIDE OF THE BIOLOGICAL SHIELD OF THE GENEVA ARGONAUT

Direction	Source of Gamma Rays	Gamma-ray Energy, Mev	ϕ_γ, r/hr	ϕ_f, n/(cm^2)(sec)	ϕ_s, n/(cm^2)(sec)
Thermal column	Graphite capture	5	0 002		
	Heavy concrete capture	6	0 007		
	Heavy concrete capture	8	0 013		
	Other	-	0 001		
	Total		0 023	$4\ 93 \times 10^{-1}$	$5\ 82 \times 10^{-1}$
Side of Reactor	Ordinary concrete capture	6	0 024		
	Heavy concrete capture	6	0 004		
	Heavy concrete capture	8	0 012		
	Ordinary concrete capture	8	0 009		
	Other	-	0 003		
	Total		0 052	$7\ 27 \times 10^{0}$	$3\ 12 \times 10^{1}$
Top of Reactor	Heavy concrete capture	4	0 003		
	Heavy concrete capture	6	0 012		
	Heavy concrete capture	8	0 020		
	Laminated[a] capture	8	0 006		
	Other	-	0 022		
	Total		0 063	$8\ 87 \times 10^{1}$	$1\ 93 \times 10^{2}$
Water Tank	Core fission	4	1 0		
	Inside tank[b] capture	6	14 2		
	Inside tank[b] capture	8	75 5		
	Other	-	5 3		
	Total		96 0	$5\ 00 \times 10^{-2}$	$1\ 01 \times 10^{-1}$

[a] Refers to Masonite and iron

[b] Refers to inside wall of water tank

*Note that the fast group is defined to be the removal-theory flux.

Table III

GAMMA-RAY DOSE RATES AND NEUTRON FLUXES AT THE OUTSIDE OF THE BIOLOGICAL SHIELD OF ARGONAUT-I

Direction	Source of Gamma Rays	Gamma-ray Energy, Mev	ϕ_γ, r/hr	ϕ_f, n/(cm^2)(sec)	ϕ_s, n/(cm^2)(sec)
Thermal column:	Graphite capture	2	0.05		
	Graphite capture	5	2.40		
	Other	-	0.12		
	Total		2.57	1.0×10^3	1.7×10^3
Side of Reactor:	Concrete capture	4	0.023		
	Concrete capture	6	0.138		
	Concrete capture	8	0.068		
	Other	-	0.005		
	Total		0.234	1.4×10^1	8.5×10^1
Top of Reactor:	Water capture	2	0.056		
	Core fission	4	0.100		
	Heavy concrete capture	4	0.022		
	Heavy concrete capture	6	0.073		
	Core fission	6	0.027		
	Heavy concrete capture	8	0.126		
	Laminated[a] capture	8	0.064		
	Other	-	0.080		
	Total		0.548	1.7×10^3	3.1×10^3
Water Tank:	Core fission	4	3.6		
	Inside tank[b] capture	4	9.5		
	Graphite capture	5	4.3		
	Core fission	6	1.3		
	Inside tank[b] capture	6	37.8		
	Inside tank[b] capture	8	176		
	Other	-	1.5		
	Total		234.0	1.6×10^0	3.6×10^0

[a]Refers to Masonite and iron region

[b]Refers to inside wall of water tank

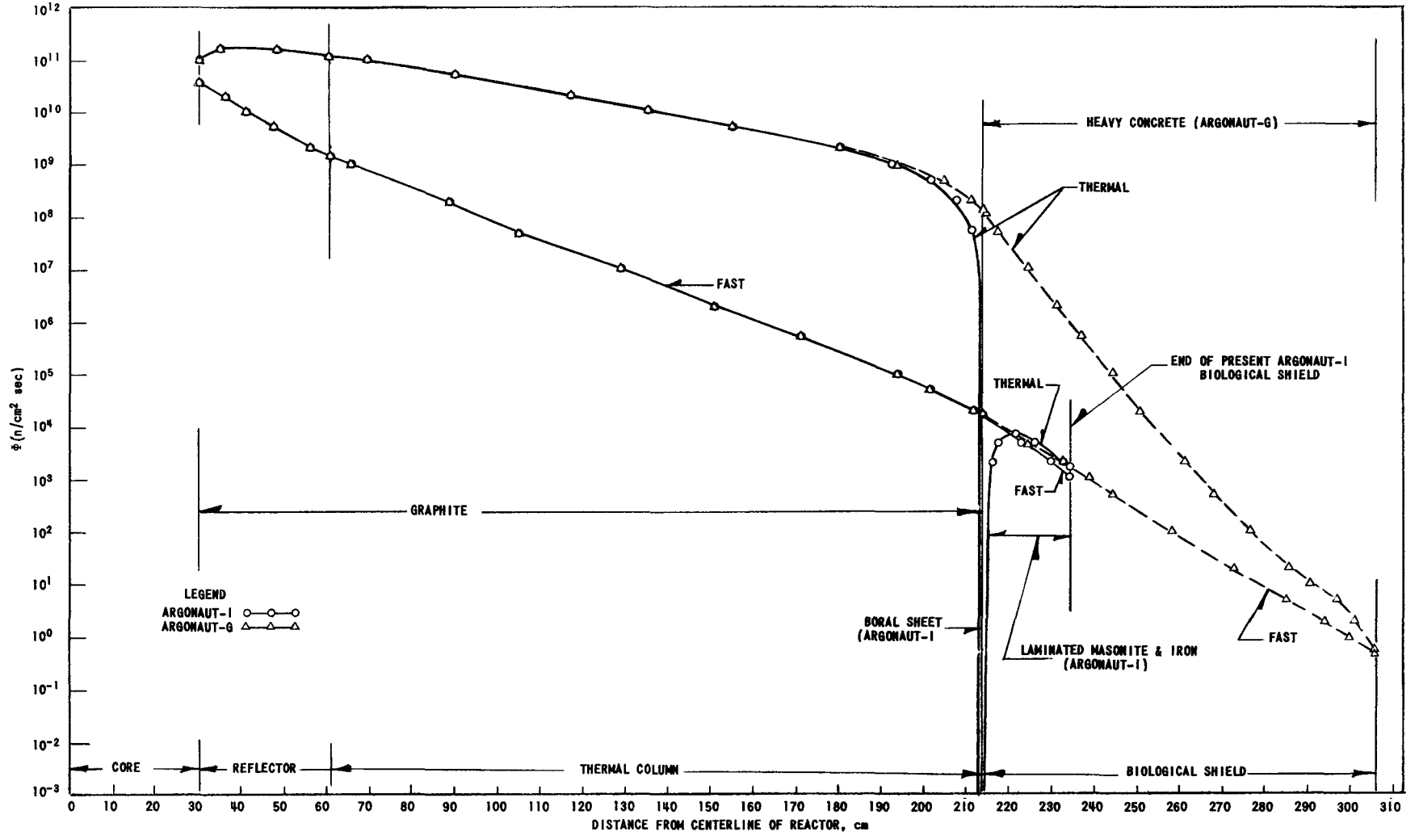

FIG. 4
NEUTRON FLUXES - THERMAL COLUMN

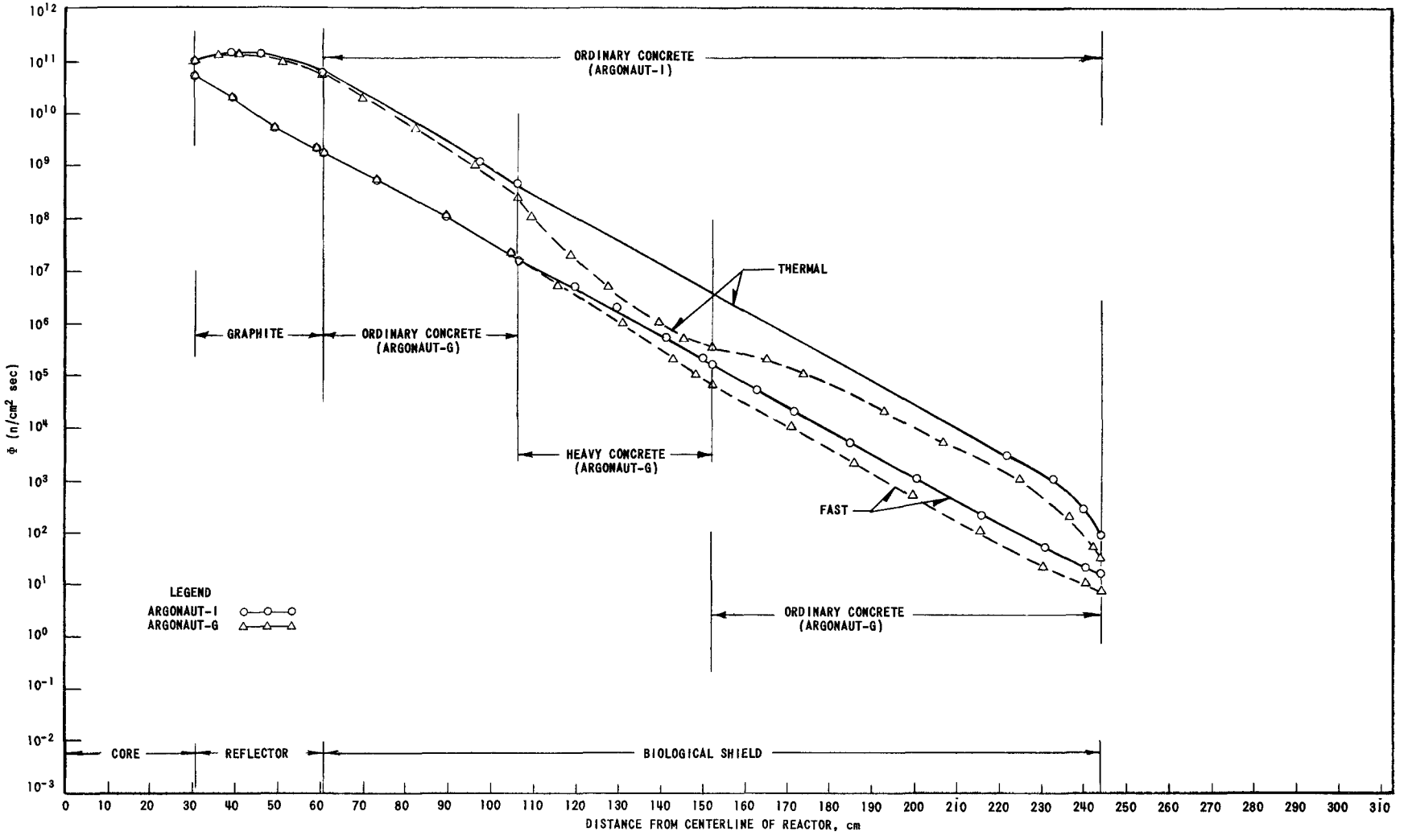

FIG. 5
NEUTRON FLUXES - SIDE OF THE REACTOR

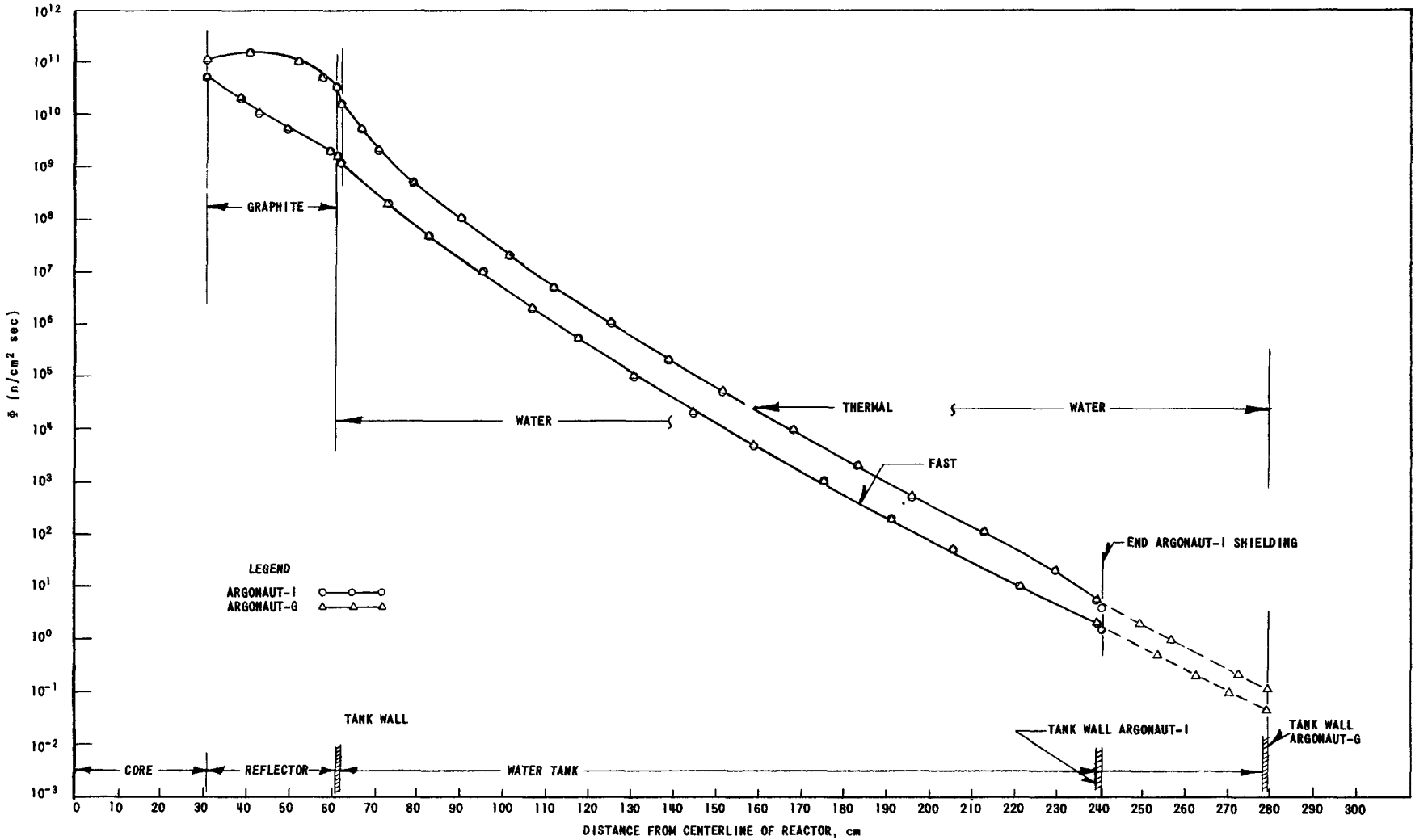

FIG. 6
NEUTRON FLUXES - WATER TANK

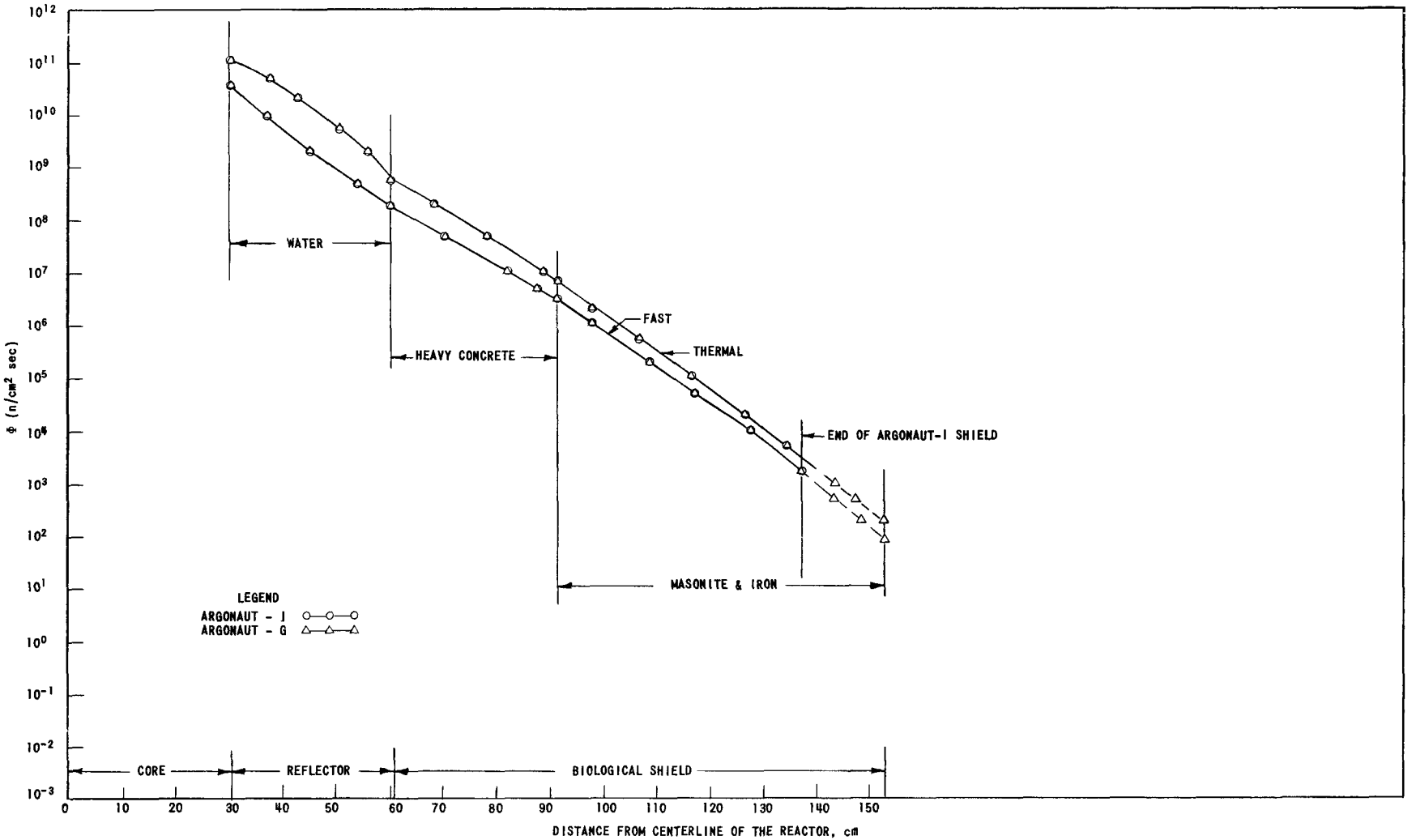

FIG. 7
NEUTRON FLUXES - TOP OF THE REACTOR

EXPERIMENTAL RESULTS

Although the Argonaut-I reactor has been operating for more than two years, no complete shield survey has been made at a known power level and with the core in all three positions for which the calculations were done. This was primarily due to the difficulty in obtaining an accurate power calibration at the low power levels of normal operation. The power calibration which has been used for this report was calculated from the thermal neutron flux distribution in the core, since not enough energy is released to obtain accurate measurements of the heating rate for the core. Therefore, the measurements that have been made cannot be related to the power with any better accuracy than a factor of 1.5. In addition, all of the surveys that have been reported were done for a one-slab loading on the side of the annulus nearest the thermal column. Therefore, the geometrical arrangement in which the measured results were obtained corresponds to the calculated situations only in the thermal column and top shield directions. Another correction should have been made to compare the results in the direction of the water tank since, for normal operation, slabs of iron were placed in the water tank. The same corrections which apply to the Argonaut-I measurements must also be made to the Geneva-Argonaut measurements before they can be compared with the calculated results for that reactor.

In spite of these limitations in the experimental measurements, it was felt that the inclusion of the most accurate results available was essential to the usefulness of this report. Therefore, in Table IV and V are shown measured dose rates, fast neutron fluxes, and thermal neutron fluxes at the outside of the biological shield on the core centerline.

Table IV

MEASURED RESULTS FOR ARGONAUT-I[a]

Direction	ϕ_γ, r/hr	ϕ_f, n/(cm^2)(sec)	ϕ_s, n/(cm^2)(sec)
Thermal Column	5.65	1.22×10^4	6.52×10^4
Side Shield	0.043	1.36×10^2	1.65×10^2
Top Shield	0.522	6.00×10^3	1.96×10^3
Water Tank[b]	0.234	2.72×10^2	7.83×10^2

[a] Measurements made with one-slab loading on thermal column side.

[b] Measured with 7 in. of iron at outside of water tank.

Table V

MEASURED RESULTS FOR THE GENEVA ARGONAUT[a]

Direction	$\phi\gamma$, mr/hr	ϕ_f, n/(cm²)(sec)	ϕ_s, n/(cm²)(sec)
Thermal Column	15	0	0
Side Shield	38	0	0
Top Shield[b]	<250	<300	<300
Water Tank[c]	14	0	0

[a] Zero readings in the table to be interpreted as essentially zero at ~500 watts.

[b] Top shield readings known to be high due to streaming from a crack.

[c] Reading made with 8 in. of iron distributed in tank.

CONCLUSION

The Argonaut shields were never completed for 10-kw operation; these shields were to be added after a period of operation. The type of operation for which the Argonaut was used, namely, for routine, low-power training, never required the additional shielding to be placed. This study was conducted to learn what amount of additional shielding would be necessary, or what the maximum operating level could be. The maximum allowable average thermal flux in the core for operation of the Argonaut-I (this assumes a one-slab loading on the thermal column side) such that the dose rate at the outside of the biological shield would not exceed 7.5 mr/hr would be approximately 1×10^8 n/(cm^2)(sec). The comparable flux for the Geneva Argonaut Reactor would be approximately 2×10^{10} n/(cm^2)(sec). Here 1×10^{11} n/(cm^2)(sec) $\cong$ 10 kw for a one-slab loading.

The second result which it was hoped could be obtained for this study was an estimate of the overall accuracy of the methods used in this analysis. For this purpose a comparison has been made of the calculated gamma-ray dose rates with those measured values which most accurately fit the geometry and assumptions made in the calculations. The gamma-ray dose rates at the outside of the biological shield were used in this analysis for several reasons. First, the accuracy of the gamma-ray measurements was better than that of the neutron fluxes; second, the gamma-ray dose rates were the determining factor as far as the shield thickness was concerned; and third, the thermal neutron flux distributions were reflected in the gamma-ray values since the major portion of the dose was due to capture gamma rays.

The results from Table VI show that the calculated results were pessimistic by something less than a factor of two, except in the case of the thermal column of the Argonaut-I. Several facts indicate that the calculated results in that direction are questionable. These data seem to be in error due to the facts that the calculated result was less than the measured dose rate and the methods used were such that a pessimistic estimate should definitely have resulted. Since the graphite used

Table VI

COMPARABLE MEASURED AND CALCULATED RESULTS FOR THE ARGONAUT REACTORS

Direction	Calculated mr/hr	Measured mr/hr
Thermal Column, Argonaut-I	2600	5600
Thermal Column, Geneva Argonaut	23	15
Top Shield, Argonaut-I	550	520

in the thermal column of Argonaut-I was obtained from CP-2, a good explanation of the discrepancy is that the impurities in the graphite of the thermal column made a significant contribution to the capture gamma-ray source. This explanation is upheld by a chemical analysis of similar graphite (also from CP-2), which showed significant amounts of vanadium (300-400 ppm), calcium (150 ppm), silicon (50 ppm), sodium (20-30 ppm), and iron (10-15 ppm) in addition to minute quantities of many other elements. The presence of these impurities in the graphite will obviously have a dual effect on the results. The thermal flux will be decreased due to the increased absorption; however, the capture gamma-ray sources will be increased. The actual change in the thermal flux due to the increased absorption should not be large, since a constant buckling correction represents a significant portion of the loss of neutrons in the thermal column. The increased capture rate will provide a significant contribution to the dose rate at the outside of the shield since the capture in some of the impurities yields gamma rays of notably higher energy than the capture in graphite. Thus, the calculations do provide slightly pessimistic results in all the comparable cases from which shield thicknesses can be predicted adequately.

ACKNOWLEDGEMENTS

I would like to express my sincerest gratitude to Marshall Grotenhuis, under whose direction this work was done. In addition, many thanks are due A. E. McArthy and A. D. Rossin for their able consultation, and to D. Daavettila and J. H. Dunlap for their aid in obtaining the experimental data.

The shield design work for the Argonaut-I was done by A. Selep* but was not formally reported. The calculational methods used at that time have been somewhat altered.

*Allis-Chalmers Mfg Co., Milwaukee

REFERENCES

1. Armstrong, R. H., and C. N. Kelber, Argonaut - Argonne's Reactor for University Training, Nucleonics 15 (3), 62-65 (March 1957).
2. Lennox, D. H., and C. N. Kelber, Summary Report on the Hazards of the Argonaut Reactor, ANL-5647 (December 1956).
3. Proceedings of the Second United Nations International Conference on the Peaceful Uses of Atomic Energy, Geneva (1958), Vol. 10, p. 265.
4. Davis, M. V., and D. T. Hauser, Thermal Neutron Data for the Elements, Nucleonics, 16 (3), 87-89 (March 1958).
5. Chapman, G. T., and C. L. Storrs, Effective Neutron Removal Cross Sections for Shielding, AECD-3978 (ORNL-1843) (September 19, 1955).
6. Reactor Physics Constants, (R. Avery, Editor) ANL-5800 (July 1958), p. 477.
7. Gladys White Grodstein, X-Ray Attenuation Coefficients from 10 kev to 100 Mev, NBS Circular 583 (April 30, 1957), Ch. 1-3.
8. See Ref. 6, p. 472.
9. Goldstein, H., and J. E. Wilkins, Jr., Calculations of Penetrations of Gamma Rays - Final Report, NYO-3075 (June 30, 1954).
10. Albert, R. D., and T. A. Welton, A Simplified Theory of Neutron Attenuation and its Application to Reactor Shield Design, WAPD-15 (Nov. 30, 1950).
11. Grotenhuis, M., Lecture Notes on Reactor Shielding, ANL-6000 (March 1959), p. 88.
12. Reactor Shielding Design Manual, (T. Rockwell, III, Editor) TID-7004, McGraw-Hill and D. Van Nostrand (March 1956), p. 360.
13. See Ref. 8, p. 463.
14. See Ref. 12, p. 348.
15. See Ref. 11, p. 99.
16. See Ref. 15, p. 102.
17. Butler, M., and J. Cook, A Reactor Shielding Program for the 704, ANL-5859.
18. See Ref. 6.
19. See Ref. 12, p. 42.